

# HARVESTING THERMAL FLUCTUATIONS: ACTIVATION PROCESS INDUCED BY A NONLINEAR CHAIN IN THERMAL EQUILIBRIUM

Ramon Reigada\*

Department of Chemistry and Biochemistry 0340  
University of California, San Diego  
La Jolla, California 92093-0340

Antonio Sarmiento†

Department of Chemistry and Biochemistry 0340  
University of California, San Diego  
La Jolla, California 92093-0340

Aldo H. Romero‡

Department of Chemistry and Biochemistry 0340  
and Department of Physics  
University of California, San Diego  
La Jolla, California 92093-0340

J. M. Sancho

Departament d'Estructura i Constituents de la Matèria  
Universitat de Barcelona  
Avda. Diagonal 647, 08028 Barcelona, Spain

Katja Lindenberg

Department of Chemistry and Biochemistry 0340  
and Institute for Nonlinear Science  
University of California San Diego  
La Jolla, California 92093-0340

October 27, 2018

## Abstract

We present a model in which the immediate environment of a bistable system is a molecular chain which in turn is connected to a thermal environment of the Langevin

---

\*Permanent address: Departament de Química-Física, Universitat de Barcelona, Avda. Diagonal 647, 08028 Barcelona, Spain

†Permanent address: Instituto de Astronomía, Apdo. Postal 70-264, Ciudad Universitaria, México D. F. 04510, México

‡Present address: Max-Planck Institut für Festkörperforschung, Heisenbergstr. 1, 70569 Stuttgart, Germany

form. The molecular chain consists of masses connected by harmonic or by anharmonic springs. The distribution, intensity, and mobility of thermal fluctuations in these chains is strongly dependent on the nature of the springs and leads to different transition dynamics for the activated process. Thus, all else (temperature, damping, coupling parameters between the chain and the bistable system) being the same, the hard chain may provide an environment described as diffusion-limited and more effective in the activation process, while the soft chain may provide an environment described as energy-limited and less effective. The importance of a detailed understanding of the thermal environment toward the understanding of the activation process itself is thus highlighted.

## 1 Introduction

The search for mechanisms that may induce the spontaneous localization of vibrational energy in molecular materials has surfaced in a variety of contexts where such localized energy may then trigger other events. These may include switching and other threshold phenomena, chemical reactions, local melting and other deformational effects, and even detonation. In the Kramers problem<sup>1,2</sup> a particle moving in a bistable potential is used as a model for a chemical process. The trajectory of the particle is associated with the reaction coordinate (RC). One well of the bistable potential represents the “reactant” state, the other the “product” state, and separating them is the “activation barrier.” The bistable potential is connected to a thermal environment, typically through fluctuating and dissipative terms, and every once in a while a large thermal fluctuation causes the particle to surmount the barrier and move from one well to the other. The average rate of occurrence of these events is associated with the reaction rate. This mesoscopic Langevin-type of approach admits of an underlying microscopic description of the thermal environment and its coupling to the bistable system. For instance, the usual Langevin equation with an instantaneous dissipation and Gaussian  $\delta$ -correlated fluctuations can be derived from a picture in which the system is harmonically coupled to an infinite number of harmonic oscillators with a uniform spectrum. A generalized Langevin picture involving dissipative memory terms and correlated fluctuations is associated with a more complex spectrum.<sup>3</sup> It is clear, and has become a topic of considerable interest, that the nature of the environment and its coupling to the bistable system profoundly influence the transition rate.

A different but related set of problems that has attracted intense interest in recent years concerns the spontaneous localization of vibrational energy in periodic nonlinear arrays. The pioneering work of Fermi, Pasta and Ulam<sup>4</sup> demonstrated that a periodic lattice of coupled nonlinear oscillators is not ergodic, and that energy in such a lattice may never be distributed uniformly. A great deal of work has since followed in an attempt to understand how energy is distributed in discrete nonlinear systems.<sup>5-17</sup> The existence of solitons and more generally of breathers and other energy-focusing mechanisms, and the stationarity or periodic recurrence or even slow relaxation of such spatially localized excitations, are viewed as nonlinear phenomena with important consequences in many physical systems.<sup>13,18,19</sup> The search for localization mechanisms that are robust even when the arrays are in a thermal environment<sup>13,15,16,20</sup> has, on the one hand, narrowed the problem (because some localization mechanisms are fragile against thermal fluctuations) but on the other hand broadened it (because new entropy-driven localization mechanisms become possible). Thermal effects may be particularly important in biophysical and biochemical applications at the molecular level.<sup>21-23</sup>

The interest in the distribution and motion of energy in *periodic* arrays arises in part because localized energy in these systems may be *mobile*, in contrast with systems where energy localization occurs through disorder. Localized energy that moves with little or no dispersion may appear at one location on an array and may then be able to move to another where it can be used in a subsequent process. Traditional harmonic models suffer from the fact that dispersion thwarts such a mechanism for energy transfer. There has been a surge of recent activity in an attempt to understand the thermal conductivity of nonlinear chains<sup>24-26</sup>

The connection between the study of perfect nonlinear arrays and the Kramers problem arises because such arrays may themselves serve as models for a heat bath for other systems connected to them.<sup>27-29</sup> Albeit in different contexts, “perfect” arrays serving as energy storage and transfer assemblies for chemical or photochemical processes are not uncommon,<sup>30-33</sup> and literature on the subject goes back for two decades.<sup>34-36</sup> We thus consider the following variant of the Kramers problem: a bistable system connected to a nonlinear chain, which is in turn connected to a heat bath in the usual Langevin manner (see Fig. 1). The bistable system is only connected to the environment through its embedding in the nonlinear chain, and therefore the ability of the chain to spontaneously localize thermal energy and perhaps

to transport it to the location of the bistable system can profoundly affect the transition rate. We investigate the behavior of this model for different types of anharmonic chains and thereby establish the important role of the nature of the environment on these chemical model systems.

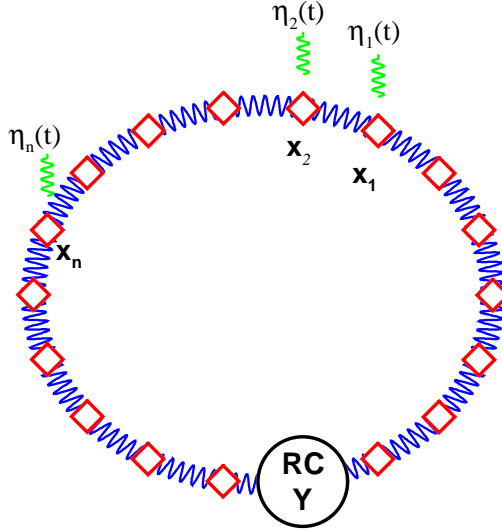


Figure 1: Schematic of a bistable impurity (“reaction coordinate” RC) connected to a chain that interacts with a heat bath at temperature  $T$ . The chain masses are indicated by rhombuses. Their interactions (shown schematically as springs) may be harmonic or anharmonic. Each mass in the chain is subject to thermal fluctuations denoted by  $\eta$  and the usual accompanying dissipation. The bistable impurity interacts only with the chain, which thus provides its thermal environment. The bistable system is inserted in the chain; its detailed interaction with the chain is discussed in the text.

In Section 2 we discuss the energy landscape typical of various nonlinear chains in thermal equilibrium. In Section 3 the variant of the Kramers problem wherein a bistable system is connected to each of the different chains is presented. Section 4 details our results for the transition statistics in the bistable system. We compare and contrast the transition statistics in the different chains and compare them to those found in the standard (Markovian) Kramers and generalized Kramers problems. We conclude with a summary and some notes on future directions in Section 5.

## 2 Nonlinear Chains

The simplest nonlinear periodic arrays consist of masses connected by springs that may be harmonic or anharmonic. The masses may also experience a local harmonic or anharmonic potential. In a recent paper we presented a detailed view of the thermal landscape of arrays with local hard (the “ $\phi^4$  model”), harmonic, or soft potentials and harmonic interactions.<sup>20</sup> Here we present the complementary analysis (more interesting, it turns out, in the context of the Kramers problem) of the thermal landscape of masses connected by anharmonic springs (with no local potentials).

The spontaneous localization of energy in any system in thermal equilibrium is simply a reflection of the thermal fluctuations described by statistical mechanics and is unrelated to system dynamics. On the other hand, the way in which these fluctuations dissipate and/or move and disperse, that is, the temporal evolution of thermal fluctuations, is dictated by the system dynamics and, in particular, by the channels connecting the chain to the thermal environment (dissipation) and the masses to one another (intermolecular interactions).

We pose the following questions: 1) How is the energy distributed in an equilibrium nonlinear chain at any given instant of time, and how does this distribution depend on the anharmonicity? Can one talk about *spontaneous energy localization* in thermal equilibrium, and, if so, what are the mechanisms that lead to it? 2) How do local energy fluctuations in such an equilibrium array relax in a given oscillator? Are there circumstances in the equilibrium system wherein a given oscillator remains at a high level of excitation for a long time? 3) Can local high-energy fluctuations move in some nondispersive fashion along the array? Can an array in thermal equilibrium transmit long-lived high-energy fluctuations from one region of the array to another with little dispersion?

In our earlier work<sup>20</sup> we showed that in harmonically coupled nonlinear chains (“diagonal anharmonicity”) in thermal equilibrium, high-energy fluctuation mobility does *not* occur beyond that which is observed in a harmonic chain. Herein we show that the situation might be quite different if there is “nondiagonal anharmonicity,” that is, if the interoscillator interactions are anharmonic.

Our model consists of a one-dimensional array of  $N$  unit-mass sites, each connected by

a potential  $V(x_n - x_{n\pm 1})$  to its nearest neighbors that may be harmonic or anharmonic:

$$H = \sum_{n=1}^N \frac{p_n^2}{2} + \sum_{n=1}^N V(x_n - x_{n-1}) . \quad (1)$$

We assume periodic boundary conditions and consider three prototype potentials:

$$V_h(x) = \frac{1}{2}kx^2 + \frac{1}{4}k'x^4 \quad \text{hard}, \quad (2)$$

$$V_0(x) = \frac{1}{2}kx^2 \quad \text{harmonic}, \quad (3)$$

$$V_s(x) = \frac{k}{k'} \left[ |x| - \frac{1}{k'} \ln(1 + k'|x|) \right] \quad \text{soft}. \quad (4)$$

At small amplitudes the three potentials are harmonic with the same force constant  $k$ . The independent parameters  $k$  and  $k'$  allow control of the harmonic component and the degree of anharmonicity of the chain. Elsewhere<sup>38</sup> we have argued that the overarching characteristic of anharmonic oscillators is the dependence of frequency on energy. For a harmonic oscillator the frequency is  $\sqrt{k}$  independent of energy; for a hard oscillator the frequency increases with energy, and for a soft oscillator the frequency decreases with energy.

The set of coupled stochastic equations of motion for the masses is that obtained from the Hamiltonian, Eq. (1), augmented by the usual Langevin prescription for coupling a system to a heat bath at temperature  $T$ :

$$\ddot{x}_n = -\frac{\partial}{\partial x_n} [V(x_{n+1} - x_n) + V(x_n - x_{n-1})] - \gamma \dot{x}_n + \eta_n(t) , \quad (5)$$

where a dot represents a derivative with respect to time. The  $\eta_n(t)$  are mutually uncorrelated, zero-centered, Gaussian,  $\delta$ -correlated fluctuations that satisfy the fluctuation-dissipation relation  $\langle \eta_n(t) \eta_j(t') \rangle = 2\gamma k_B T \delta_{nj} \delta(t - t')$ . The numerical integration of the stochastic equations for all our simulations is performed using the second order Heun's method (which is equivalent to a second order Runge Kutta integration)<sup>39,40</sup> with time step  $\Delta t = 0.005$ . In each simulation the system is initially allowed to relax for enough iterations to insure thermal equilibrium, after which we take our "measurements."

The equilibrium results to be presented here complement our observations, presented elsewhere, on the way in which these same chains propagate an energy pulse<sup>38</sup> as well as a sustained signal applied at a particular site.<sup>41</sup>

A set of energy landscapes is shown in Fig. 2. Along the horizontal direction in each panel lies a thermalized chain of oscillators; the vertical upward progression shows the evolution of this equilibrium system with time. The gray scale represents the energy, with darker shading reflecting more energetic regions.

Several noteworthy features are evident in the figure. The energy fluctuations are greatest in the soft chain. This feature, seen earlier in chains with local anharmonic potentials,<sup>15,20</sup> is a consequence of the effect that we have called *entropic localization*. In the soft chain not only are the thermal fluctuations greater at a given temperature, a result easily obtained from a simple virial analysis, but the free energy is minimized by a nonuniform distribution of energy that populates regions of phase space where the density of states is high. We have argued that this localization mechanism is robust against temperature increases – indeed, it becomes more effective with increasing temperature. A second distinctive feature of the soft chain is the persistence of the energy fluctuations: damping is not particularly effective for soft chains. The only other mechanism for removal of localized energy from a particular location is along the chain. This is clearly not an effective mechanism, a result that is in agreement with our analysis of the propagation of an externally applied pulse in the soft chain.<sup>38</sup> The speed of propagation (in all chains) of a pulse of a given energy is essentially proportional to the average frequency associated with that energy, and in the soft chain this average frequency decreases with increasing energy.<sup>38</sup> Although we do not see an obvious connection between these excitations and solitons at zero temperature (which are not entropic localization mechanisms),<sup>10,17,31,33–35</sup> there may be a closer connection with more generalized excitations such as breathers.<sup>13,16,21</sup>

In the hard chain (Fermi-Pasta-Ulam chain) the total energy as well as the energy fluctuations are considerably smaller but quite mobile with little dispersion, as can easily be shown on the basis of a straightforward statistical mechanical analysis. In the hard chain the average frequency increases with energy and therefore more energetic pulses tend to travel more rapidly. We have also shown that the dispersion of energy in a hard chain is slow<sup>38</sup> – this is seen here in the integrity of the spontaneously localized pulses over a much longer time than in the harmonic chain.

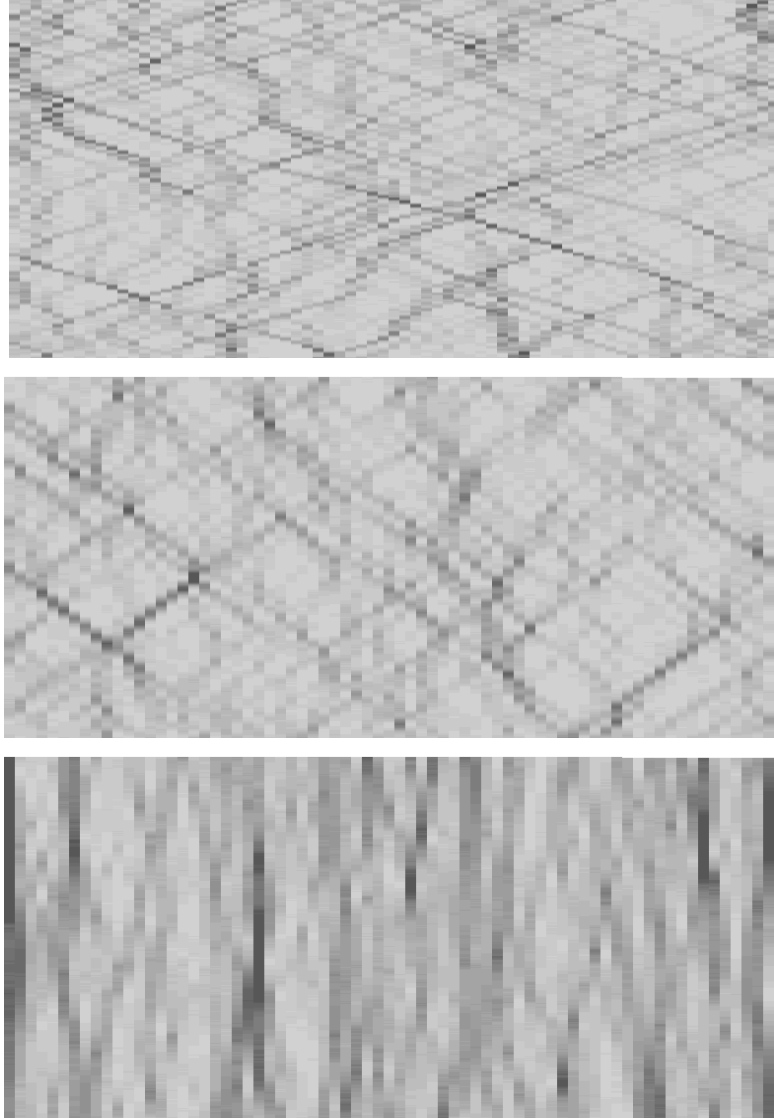


Figure 2: Energy (in grey scales) for thermalized chains of 71 oscillators as a function of time. The  $x$ -axis represents the chain and time advances along the  $y$ -axis, with  $t_{max} = 160$ . The temperature is  $k_B T = 0.08$  and the dissipation parameter is  $\gamma = 0.005$ . Top panel: hard chain with  $k = 0.1$ ,  $k' = 1$ ; middle panel: harmonic chain with  $k = 0.1$ ; lower panel: soft chain with  $k = 0.1$ ,  $k' = 5$ .

An important question of course concerns the parameter regimes where the differences illustrated in Fig. 2 are observed. We have chosen potential parameters that insure clear distinctions in the displacement amplitudes associated with the three potentials at the chosen temperature. The only restriction is that the temperature not be “too low,” that is, we avoid the region where all three potentials are essentially harmonic. We have chosen very low damping for the illustration. The soft energy landscape is far less sensitive to damping than the hard array. An increase in damping would readily slow down the motion of the high-energy fluctuations and would shorten their lifetime. Further, while the speed of the energy fluctuation pulses is sensitive to the potential parameters, their lifetime and dispersion properties are less so (as long as one is in the highly anharmonic regime). On the other hand, the persistence of the fluctuations in the soft array is quite sensitive to the harmonic contribution to the potential. All else remaining fixed, the landscapes remain qualitatively similar as temperature increases: the fluctuations in the soft array become even stronger relative to the others, and the pulse speeds in the hard array become even higher.

Suppose now that a bistable “impurity” is embedded in each of these chains, as illustrated in Fig. 1. When sufficient energy reaches the impurity, a transition may occur from one well to the other. The statistical and dynamical properties of these transitions are not obvious, and are explored in the next section.

### 3 Kramers Problem and Statement of our Variant

#### 3.1 Traditional Kramers Problem

The original Markovian Kramers problem<sup>1</sup> describes the reaction coordinate  $y$  evolving in the bistable potential

$$V_b(y) = \frac{V_0}{4}(y^2 - 1)^2 \quad (6)$$

according to the usual Langevin prescription

$$\ddot{y} = -\frac{dV_b(y)}{dy} - \gamma_b \dot{y} + \eta_b(t) \quad (7)$$

where  $\gamma_b$  is the dissipation parameter (the subscript for “bistable” distinguishes this from the other dissipation parameters) and  $\eta_b(t)$  represents Gaussian, zero-centered,  $\delta$ -correlated fluctuations that satisfy the fluctuation-dissipation relation appropriate for temperature  $T$ ,  $\langle \eta_b(t)\eta_b(t') \rangle = 2\gamma_b k_B T \delta(t - t')$ . The rate coefficient  $k_r$  for transitions from one metastable well to the other is expressed as

$$k_r = \kappa k^{TST}, \quad (8)$$

where  $k^{TST}$  is the rate obtained from transition state theory for activated crossing, which in our units ( $V_0 = 1$ , frequencies  $\sqrt{2}$  at the bottom of the two wells and unit frequency at the top of the barrier) is

$$k^{TST} = \frac{\sqrt{2}}{\pi} e^{-1/4k_B T}. \quad (9)$$

This is the highest possible rate because it assumes no recrossings of the barrier when the particle moves from one well to the other. The “transmission coefficient”  $\kappa < 1$  captures the effects of recrossings. The dependence of  $\kappa$  on the various parameters of the problem has been the subject of intense study over many years.<sup>2,42-44</sup> Its dependence on  $\gamma_b$  and temperature is exemplified in the simulations shown in Fig. 3. In particular, we note the occurrence of a maximum: as predicted by Kramers, the transmission coefficient at high friction (diffusion-limited regime) decays as  $\gamma_b^{-1}$  (and is independent of temperature); at low friction (energy-limited regime) Kramers predicted that  $\kappa$  is proportional to  $\gamma_b/k_B T$ .

An important generalization of the original Kramers problem, the so-called Grote-Hynes problem,<sup>45</sup> reformulates the model in terms of the generalized Langevin equation

$$\ddot{y} = -\frac{dV_b(y)}{dy} - \int_0^t dt' \Gamma(t - t') \dot{y}(t') + \eta_b(t) \quad (10)$$

where  $\Gamma(t - t')$  is a dissipative memory kernel and the fluctuation-dissipation relation is now generalized to  $\langle \eta_b(t)\eta_b(t') \rangle = k_B T \Gamma(t - t')$ . The dissipative memory kernel reflects the dynamics of the thermal environment and is characterized by its own time scales. A frequent choice is an exponential, but other forms that have been used include a Gaussian and a decaying oscillatory memory kernel. The introduction of additional parameters of course changes the behavior of the transmission coefficient.

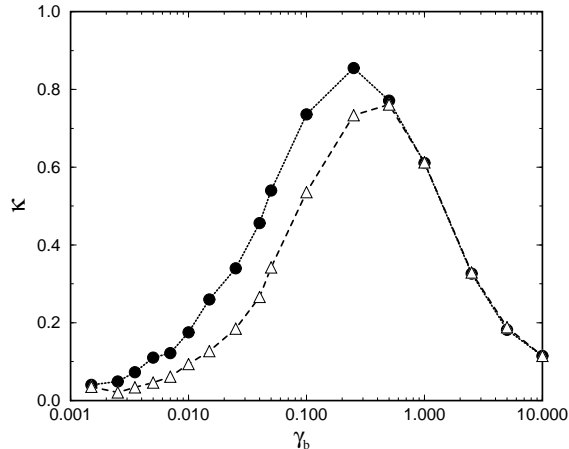


Figure 3: Transmission coefficient  $\kappa$  vs dissipation parameter  $\gamma_b$  for two temperatures obtained from direct simulation of Eq. (7). Solid circles:  $k_B T = 0.025$ ; triangles:  $k_B T = 0.05$ .

The main point here is to call attention to the fact that the transmission coefficient has the same value for two different values of the dissipation parameter  $\gamma_b$ , and that therefore one can not conclude whether the system is in one regime (diffusion-limited) or another (energy-limited) simply from the value of the transition rate. One needs to know the trend with changing dissipation parameter, and one requires further information about the dynamics underlying a given transition rate. Not surprisingly, these dynamics turn out to be entirely different in different regimes.<sup>46</sup> The time dependence of the transmission coefficient is a direct reflection of the explicit trajectories of the particle as it transits from one well to the other. A number of investigators have looked at the time dependence of the transmission coefficient in the diffusion-limited<sup>47–51</sup> and energy-limited<sup>47,49–51</sup> regimes, and also at the effect of different types of memory kernels.<sup>50–52</sup>

Of interest to us here are the different dynamical behaviors in the diffusion-limited regime and the energy-limited regime. In Fig. 4 we show two views of each of two typical trajectories of the reaction coordinate for the Markovian Kramers problem. The transmission coefficients associated with these two trajectories are not too different (see below), but

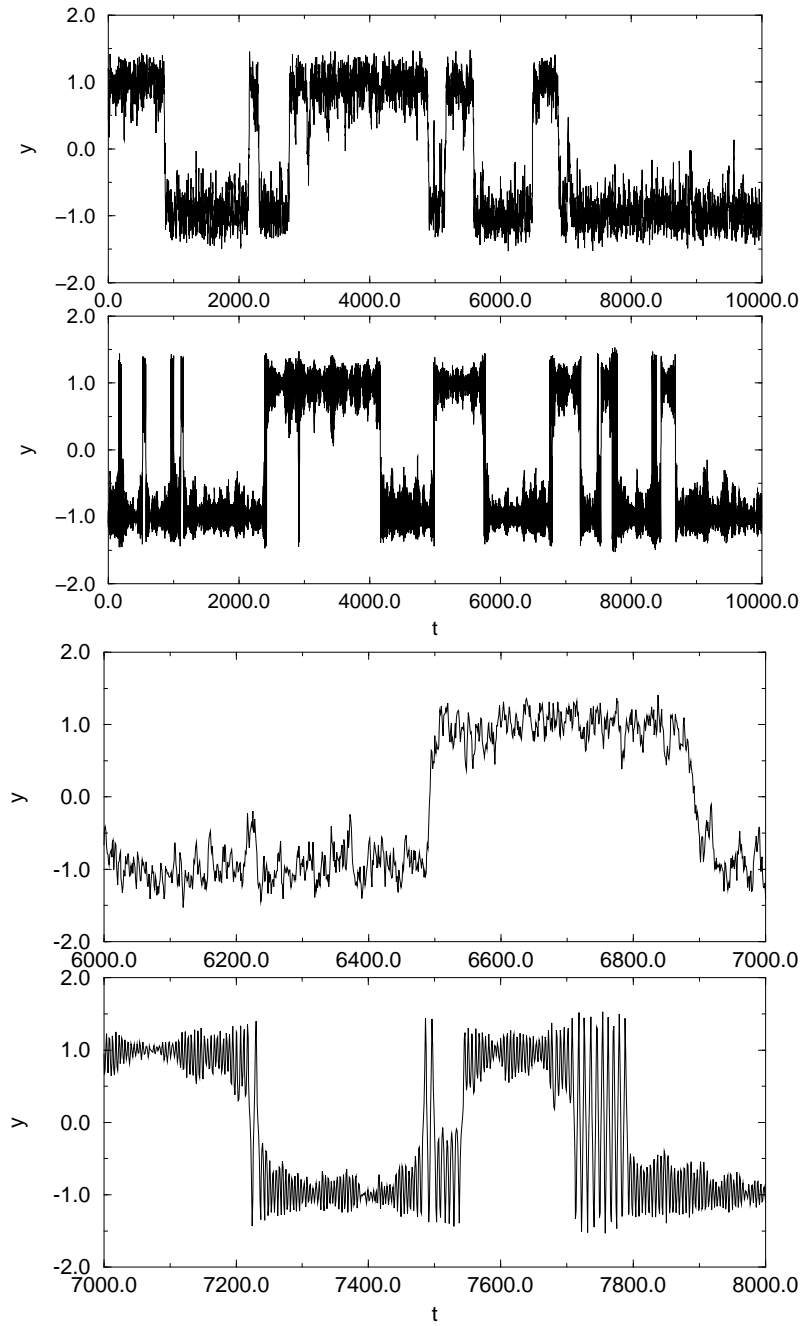


Figure 4: Trajectory of a bistable impurity described by the Langevin equation, Eq. (7). The temperature is  $k_B T = 0.08$ . First panel:  $\gamma_b = 5.0$ . Second panel:  $\gamma_b = 0.02$ . The third (fourth) panel zooms in on a portion of the high-damping (low-damping) trajectory.

they correspond to different damping, placing them on opposite sides of the turnover in the  $\kappa$  vs  $\gamma_b$  curve. The trajectory in the first panel is in the diffusion-limited regime; the third panel shows an expanded view of a portion of this trajectory. The particle performs rather erratic motion within one well and once in a while it surmounts the barrier. When the particle surmounts the barrier it does not spend much time in the barrier region before being trapped again in one or the other well. The crossing trajectories thus tend to involve only one or a very small number of crossings/recrossings. The trajectory in the second panel, a portion of which is expanded in the fourth panel, is energy-limited. The particle performs a fairly periodic motion within one well. Barrier crossing events tend to retain the particle in the barrier region for several recrossings; a phase space analysis shows that the associated trajectories are rather smooth oscillations from one side to the other of the potential well above the barrier.<sup>49</sup> Correlation functions associated with these trajectories are presented and discussed in Section 4.

### 3.2 Variant of the Kramers Problem

We would like to understand the way in which the very different thermal landscapes described in Section 2 affect the dynamics of a reaction coordinate evolving in a bistable “impurity” embedded in these environments. The connection of the bistable impurity to the thermal environment occurs only through its connection to the chain, that is, we set  $\gamma_b = 0$ .

We need to specify how the bistable system interacts with the chain. We insert the impurity along the chain between sites  $i$  and  $i + 1$  and connect it to each of these two sites (see Fig. 1). It is customary to choose a simple interaction potential with a harmonic dependence  $V_{int}(x, y) \propto (x - y)^2$  for each chain site connected to the impurity. Here  $y$  is the reaction coordinate and  $x$  stands for the coordinate of the chain site connected to the impurity. However, this interaction tends to destabilize the bistability in that it causes the neighbors to pull the bistable particle *toward* the barrier rather than toward its natural metastable states. The interaction thus lowers the barrier of the bistable impurity. Since we do not want to “bias” the problem in this way, we have chosen an interaction that instead tends to favor the already metastable states:

$$V_{int}(x, y) = \frac{k_{int}}{2} \left( \frac{y^2 - 1}{2} - x \right)^2. \quad (11)$$

Near the bistable minima (which are shifted by the interaction) the total potential for the reaction coordinate is still harmonic, and near the maximum at  $y = 0$  it is still parabolic. The barrier height is modulated by the motion of the neighbors (somewhat reminiscent of the barrier fluctuations in resonant activation problems). At large values of  $y$  the interaction hardens the bistable potential.

The equations of evolution then have the following contributions. For a site in the chain not connected to the bistable impurity we have, as before, Eq. (5). For the bistable impurity

$$\ddot{y} = -\frac{dV_b(y)}{dy} - \frac{\partial V_{int}(x_{i+1}, y)}{\partial y} - \frac{\partial V_{int}(x_i, y)}{\partial y}. \quad (12)$$

For the site to the left of the bistable impurity

$$\ddot{x}_i = -\frac{\partial V(x_i - x_{i-1})}{\partial x_i} - \frac{\partial V_{int}(x_i, y)}{\partial x_i} - \gamma \dot{x}_i + \eta_i(t) \quad (13)$$

and similarly for  $x_{i+1}$ . Comparisons are made for the same temperature, damping coefficients, and interaction parameter ( $k_{int} = 0.1$  throughout this work) varying only the nature of the chain.

Figure 5 shows trajectories of the bistable impurity embedded in each of the three chains. In the hard chain the trajectory is rather similar to that of a Markovian Kramers particle in the diffusion-limited regime, while in the soft chain it is closer to that of the energy-limited regime. This is a direct reflection of the behavior seen in Fig. 2, that is, of the fact that in the hard chain independent thermal fluctuations created elsewhere along the chain have a good chance of reaching the bistable impurity, causing erratic motion. An occasional large fluctuation causes a transition over the barrier, usually unaccompanied by recrossings: the same energy mobility that brings independent fluctuations to the impurity also makes it easy for the impurity to then lose a particular energy fluctuation back to the chain. In the soft chain, on the other hand, the particle performs fairly periodic motion within one well. Only fluctuations in the sites immediately adjacent to the impurity can excite the impurity; fluctuations originating elsewhere do not travel to the impurity. Strong fluctuations are therefore rarer but more energetic and more persistent, so transition events occur less often. However, once such a fluctuation occurs it tends to remain in that region for a long time; the reaction coordinate therefore recrosses the barrier a large number of times until it eventually loses the excess energy and is trapped again in one of the wells.

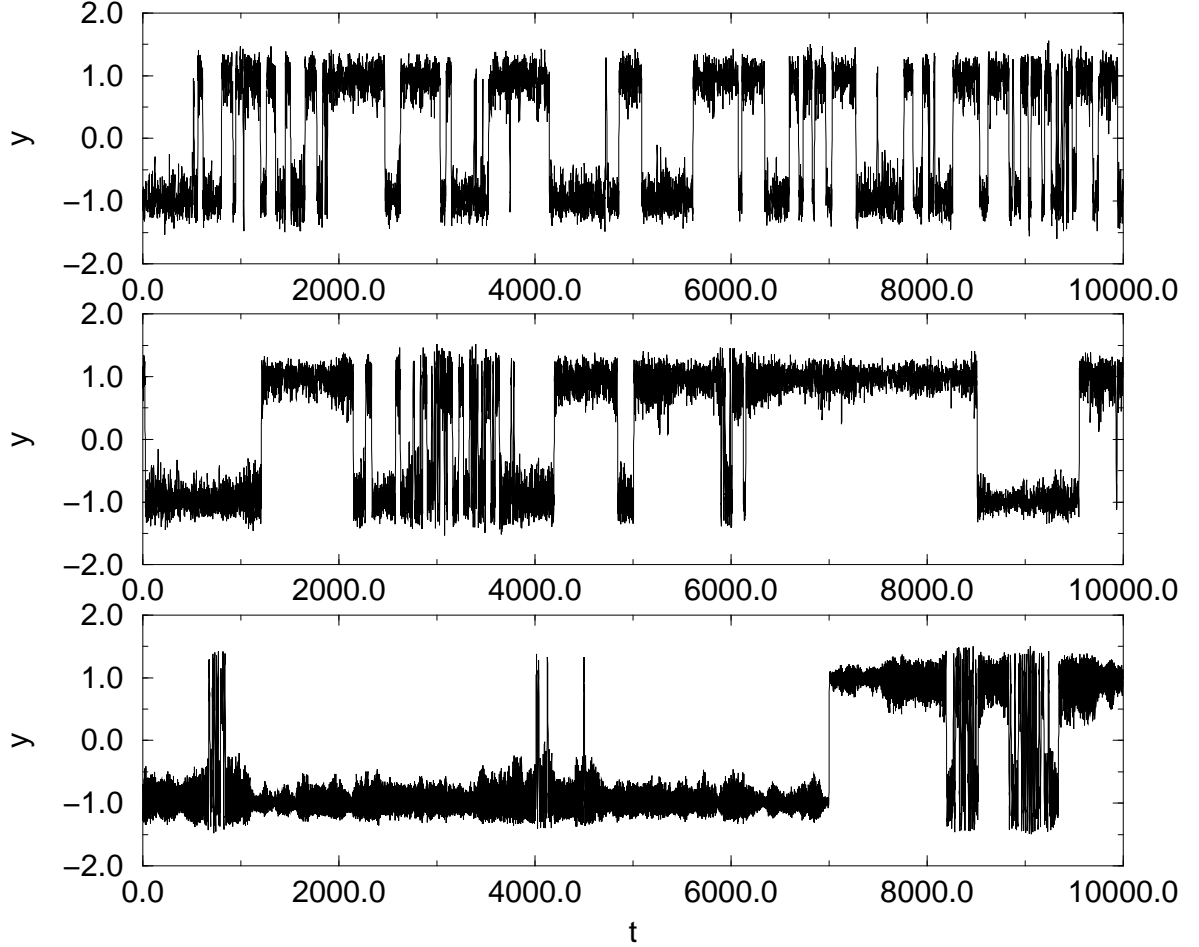


Figure 5: Trajectory of a bistable impurity embedded in a chain of 30 oscillators with  $k_B T = 0.08$  and  $\gamma = 0.005$ . Top panel: hard chain with  $k = 0.1$  and  $k' = 1$ . Middle panel: harmonic chain with  $k = 0.1$ . Bottom panel: soft chain with  $k = 0.1$  and  $k' = 5$ .

A second set of trajectories associated with the same bistable impurity in the same three chains at the same temperature but with a (10-fold) higher dissipation parameter is shown in Fig. 6. Not surprisingly, the trajectories are now more similar to one another, but nevertheless there are still important and revealing differences that will be made evident in our discussion in the next section. Furthermore, a comparison of the two sets will allow important observations concerning the trends associated with increased damping.

In the next section we provide a quantitative characterization of the differences in the trajectories and a comparison of these results with those of the traditional Kramers problem.

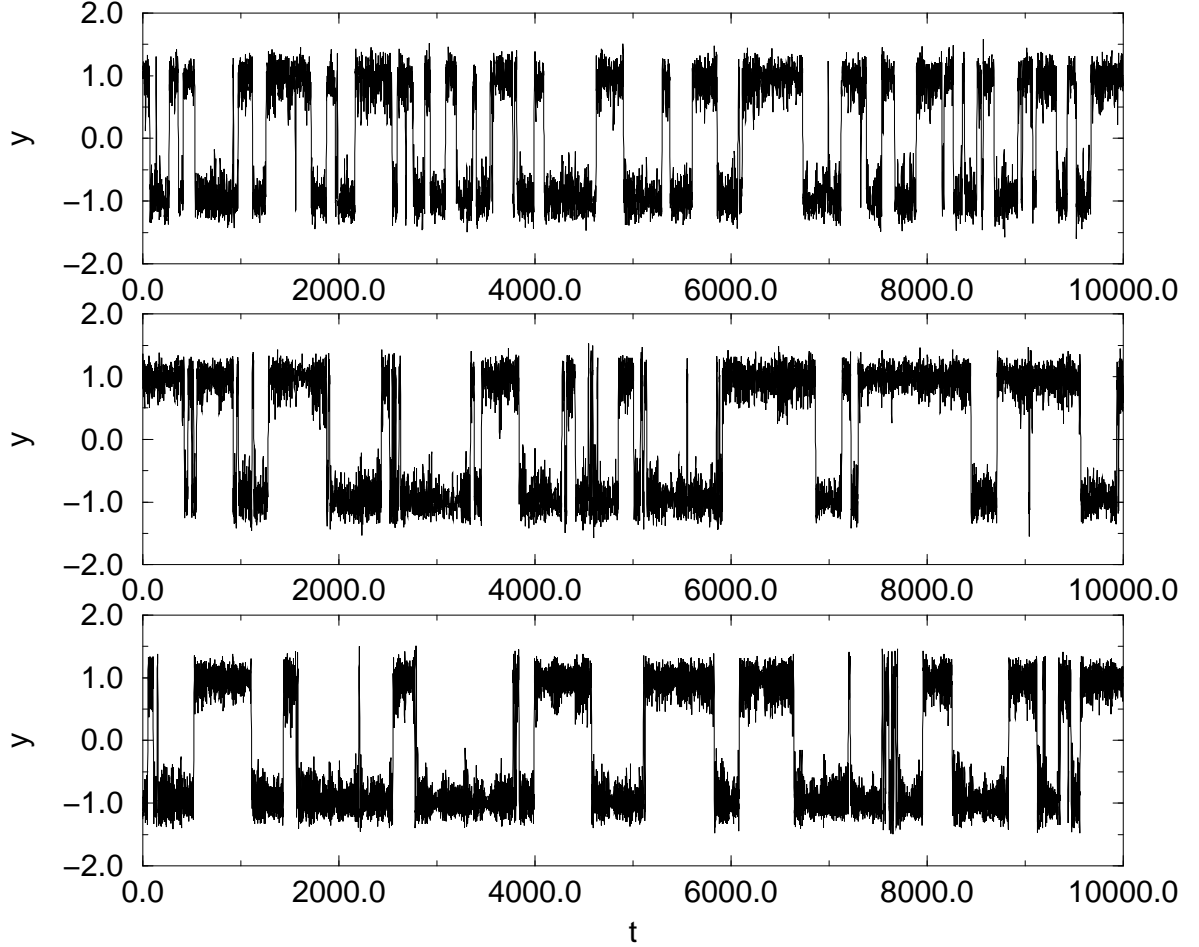


Figure 6: Trajectory of a bistable impurity embedded in a chain of 30 oscillators. All parameters are the same as in Fig. 5 except that the dissipation parameter has been increased to  $\gamma = 0.05$ .

## 4 Results for Transition Rates

A useful description of the bistable system in different regimes is provided by the normalized correlation function

$$C(\tau) \equiv \frac{\langle y(t+\tau)y(t) \rangle}{\langle y^2(t) \rangle} \quad (14)$$

where the brackets indicate an average over  $t$ . Since  $\langle y(t) \rangle = 0$ , this correlation function decays to zero. When the thermal environment strongly and rapidly changes the particle momentum, the trajectory is erratic and the correlation function decays monotonically and

exponentially. The decay time is a measure of the mean time between crossing events from one well to the other, and its inverse can be identified with the transition rate  $k_r$ . If on the other hand the effects of the thermal environment are weak, then the trajectory is determined mainly by the deterministic potential and remains correlated over much longer periods of time.

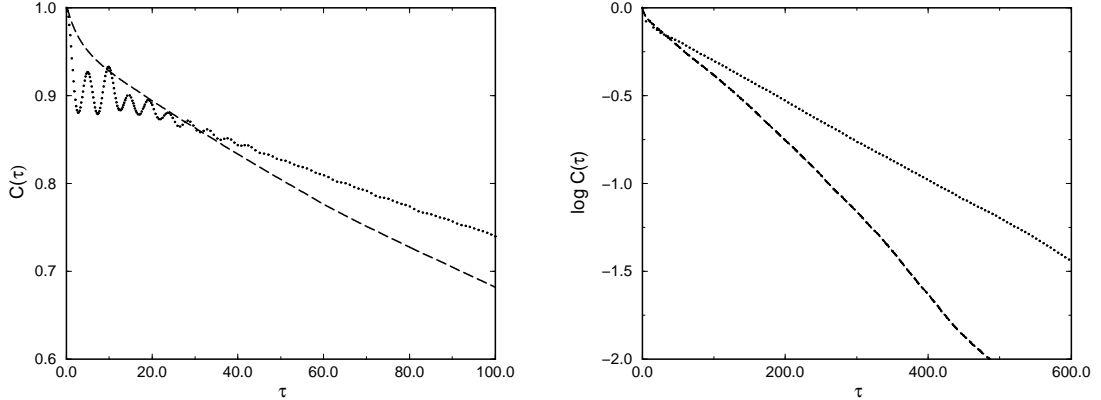


Figure 7: Correlation functions for the Markovian Kramers problem associated with the trajectories of Fig. 4. Dashed curves:  $\gamma_b = 5.0$ , dotted curves:  $\gamma_b = 0.02$ . First panel: short-time behavior. Second panel: correlation functions on a logarithmic time scale.

The correlation functions for the Markovian Kramers trajectories of Fig. 4 are shown in Fig. 7. In the high-dissipation regime the correlation function is monotonic and decays exponentially over essentially all times. This is a reflection of the essentially random motion within each well and between wells (the correlation functions for portions of the trajectory entirely within one well are also monotonically decreasing, albeit not to zero). The slope of the high- $\gamma_b$  curve in the right panel leads to a mean time between crossings of  $\tau_c \approx 250$ .

The oscillations in the low- $\gamma_b$  correlation function reflect mainly the systematic periodic motion of the particle within each well, i. e., of the portions of the trajectory that evolve for a long time near  $y = 1$  or near  $y = -1$ . The period of these oscillations for the parameters used here is  $t_{bottom} = \sqrt{2}\pi$ , and this is very nearly the period of the oscillations in the figure. Crossing events from one well to the other are mostly separated by long times and are essentially independent (however, see further discussion below). Hence the logarithmic rendition in the right panel gives a straight line. Its slope leads to a mean time between crossing events of  $\tau_c \approx 450$ .

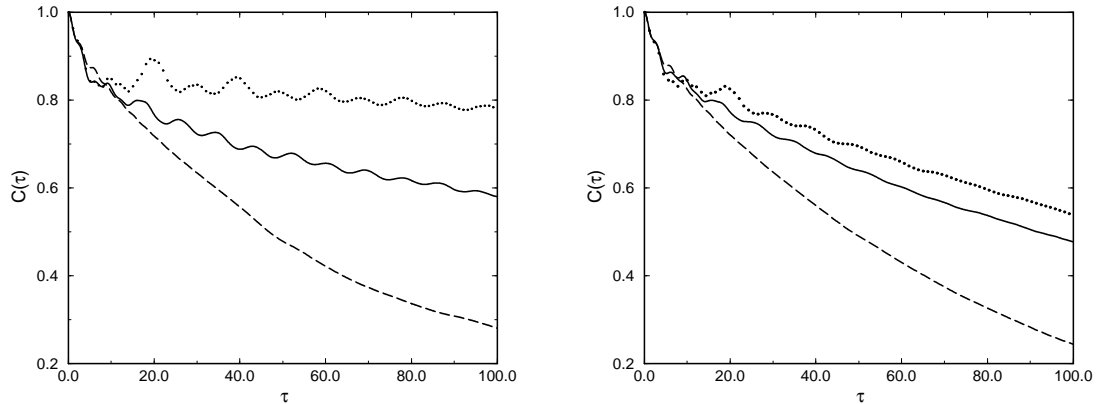


Figure 8: Correlation functions associated with the trajectories of Figs. 5 (first panel) and 6 (second panel). Dashed curves: hard chain; solid curves: harmonic chain; dotted curves: soft chain.

The Kramers correlation functions serve as a point of reference for an interpretation of the correlation functions associated with our variant of the Kramers problem. These are shown in a number of figures starting with Fig. 8, which shows the correlations functions associated with the trajectories in Figs. 5 and 6. We stress that in each panel the  $\gamma$  and  $k_B T$  are the same in all cases, as is the coupling of the chain to the bistable system; only the nature of the chain has changed. The first panel shows a correlation function for the harmonic chain that is oscillatory at early times, and quite similar to the energy-limited Markovian Kramers case (see also the corresponding trajectories in Figs. 5 and 4). We conjecture that the harmonic chain provides a thermal environment comparable to the low-damping Markovian Kramers environment. The correlation function associated with the hard chain is similar to the behavior at higher damping in the Kramers case. The correlation function associated with the soft chain also decays in an oscillatory fashion, but in a more complex way than in the energy-limited Markovian Kramers case. *The alternation in the amplitudes is a consequence of the presence of sustained bursts of energy that cause a finite fraction of the trajectory to occur above the barrier, leading to many correlated recrossing events.* The particle oscillates above the barrier for intervals much longer than in the Markovian Kramers trajectory. The typical oscillation period above the barrier is about twice as long as  $t_{bottom}$  in our example (detailed discussions of these times can be found in our earlier work<sup>49–51</sup>). This effect is already slightly visible in the low- $\gamma_b$  Kramers correlation

function in Fig. 7, but it is much stronger in the soft chain. To reproduce this behavior in the Kramers model it is necessary to consider the *generalized* Kramers model with a memory friction: there is clearly an additional memory effect in the soft chain that allows the energy to remain trapped in the region of the bistable impurity for a long time. This is in accord with the notion that transitions in the soft chain are caused by local thermal fluctuations in the nearest neighbors of the impurity. The impurity may periodically exchange energy with these neighbors before the fluctuation eventually dissipates away, and this causes repeated recrossings. This in turn leads to the conclusion that the memory friction in the Kramers model needed to reproduce the soft chain environment would most likely be oscillatory.<sup>51</sup>

The periods of oscillations in the harmonic and soft chains are somewhat different from those of the Kramers curve in Fig. 7 and from each other. This is due to differences in the effective potentials.

The eventual decay of the correlation functions for all three chains is exponential. We find for the times between transition events (single or bursts as appropriate)  $\tau_c \approx 101$  for the hard chain,  $\tau_c \approx 453$  for the harmonic chain, and  $\tau_c \approx 1540$  for the soft chain.

A similar set of correlation functions associated with the higher-damping-parameter trajectories of Fig. 6 is shown in the right panel of Fig. 8. The dynamics of the bistable system in the hard chain with increasing damping does not change in character, whereas the oscillations in the harmonic and soft chains become less pronounced as these systems move toward the diffusion-limited regime. First we note that all the curves become steeper, which translates to a *shorter* mean time between crossing events and therefore a *higher* transition rate for all three chains. The specific values we obtain are  $\tau_c \approx 72$  for the hard chain,  $\tau_c \approx 170$  for the harmonic chain, and  $\tau_c \approx 215$  for the soft chain. The decrease in time between crossing events is most pronounced for the soft chain. This is consistent with the notion that the soft chain is in the energy-limited regime where small increases in effective damping cause the greatest increases in the transition rate (see Fig. 3). The harmonic chain lies closer in this sense to the turnover region, and the hard chain even closer yet. The second point is that this apparent trend for the hard chain indicates that it, too, lies on the low-damping side of the turnover in spite of the diffusion-limited aspects of its dynamics. This is the reason for the very small oscillations visible at the earliest times in the hard chain correlation functions. It is apparent that neither the trajectory itself nor even the shape of the correlation function at one value of the damping provides unequivocal

information to determine which side of the turnover regime one is on; it is necessary to investigate the trend.

It is interesting to investigate whether our variants of the thermal environment can actually be “pushed” across the turnover point by increasing the damping on the chain. For this purpose we present a series of correlation functions for each of the chains for different values of the damping parameter. The other parameters, including the temperature, remain fixed and equal to the values given earlier.

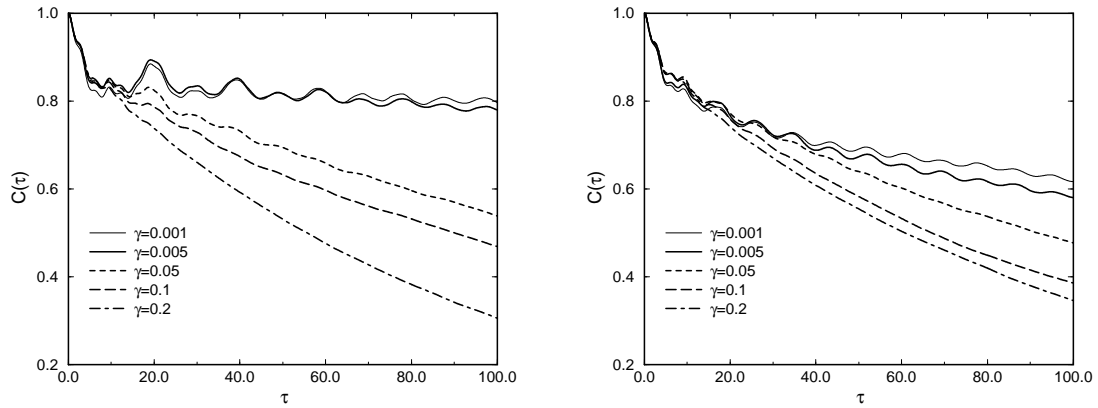


Figure 9: Correlation functions for the bistable impurity in the soft chain (first panel) and harmonic chain (second panel) or various values of the dissipation parameter.

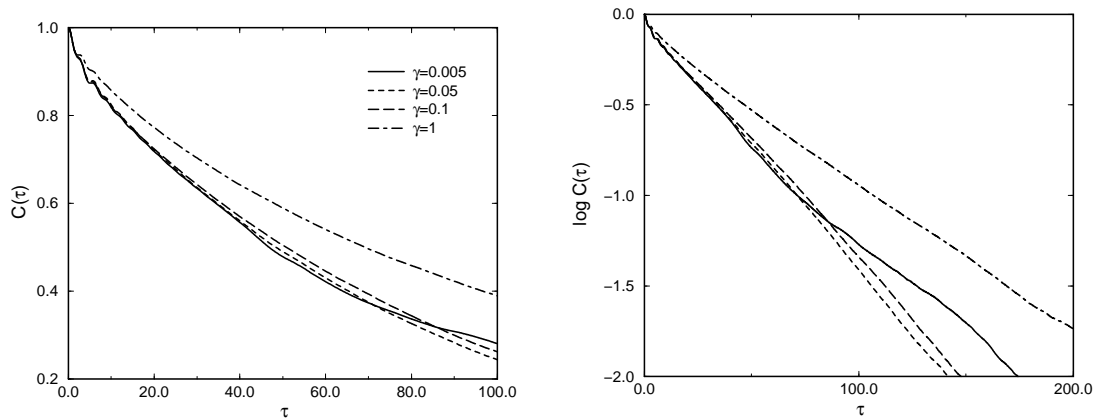


Figure 10: Correlation functions for the bistable impurity in the hard chain for various values of the dissipation parameter. First panel: short-time behavior. Second panel: correlation function on a logarithmic scale.

Figure 9 shows results for the soft and harmonic chains. With increasing damping the early-time oscillations in the correlation function in the soft chain first lose some of the “alternation” feature typical of a long oscillatory dissipative memory kernel and eventually the correlation function loses its oscillatory character altogether. The crossing rate continues to increase as damping increases, so throughout this series one is still on the low damping side of the turnover. The right panel of Fig. 9 shows the correlation functions for the impurity in the harmonic chain. The trend is similar to that of the soft chain but, in all respects, indicative of the fact that the harmonic environment is closer to the turnover region than the soft environment. Thus the oscillations disappear sooner, and the increase in the transition rate with increasing damping is smaller.

Perhaps the most interesting features are seen in Fig. 10. Here we clearly see the very small short-time oscillations, which disappear as damping increases. The transition rate is quite insensitive to damping in the range  $\gamma = 0.005 - 0.1$  shown in the figure (the line for  $\gamma = 0.2$ , not explicitly shown, also falls in the same regime). The turnover value must therefore be within this range. To ascertain if this is so, we also exhibit the correlation function for a considerably larger value of the dissipation parameter,  $\gamma = 1.0$ . The slower decay for  $\gamma = 1$  is clear in both panels.

## 5 Conclusions

There has been a dearth of information on the effects on the activation process of *nonlinearities* in the environment. We have taken an approach here that goes part way, much in the tradition of modeling efforts for a variety of systems interacting with a complex environment: the “immediate surroundings” of the reaction coordinate are described microscopically, while the interaction of this immediate environment with other degrees of freedom is handled phenomenologically.

We find that the dynamics of the activation process in some parameter regimes are profoundly affected by the nature of the chain. If the damping parameter connecting the chain to the heat bath is sufficiently low, a soft chain provides an environment very similar to that of the Grote Hynes model with an oscillatory memory kernel in the energy-limited regime,<sup>51</sup> while a hard chain provides an environment akin to that of the Kramers model in the diffusion-limited regime.<sup>49</sup> This in turn means that in such parameter regimes *the*

*hard chain is a more effective mediator of the activation process than is the soft chain.*

A number of interesting questions concerning these systems are currently under investigation. One concerns the influence of boundary conditions on the behavior that we have described.<sup>37</sup> A second problem concerns the effect on the reaction coordinate of a pulse or a sustained signal applied somewhere else along the chain. We have showed that the propagation of such a pulse or signal is strongly affected by the nature of the chain,<sup>38,41</sup> and we expect these differences in turn to affect the response of a bistable impurity to these excitations. Such models are interesting in the context of physical or biophysical situations wherein energy is released at some location (provided perhaps by a chemical reaction or an absorption process at that location), which must then move to another location (that of the bistable impurity) to effect some further chemical process (represented by the activation process). The usual linear chain models are plagued by the excessive dispersion that would make such transmission inefficient. Nonlinearities in the environment may provide the necessary mobility with little attendant dispersion, thus greatly increasing the efficiency of such a process.

## Acknowledgments

R. R. gratefully acknowledges the support of this research by the Ministerio de Educación y Cultura through Postdoctoral Grant No. PF-98-46573147. A. S. acknowledges sabbatical support from DGAPA-UNAM. This work was supported in part by the Engineering Research Program of the Office of Basic Energy Sciences at the U.S. Department of Energy under Grant No. DE-FG03-86ER13606, and in part by the Comisión Interministerial de Ciencia y Tecnología (Spain) Project No. DGICYT PB96-0241.

## References

- [1] H.A. Kramers, *Physica* **7**, 284 (1940).
- [2] For reviews of the Kramers problem see V. I. Melnikov, *Phys. Report* **209**, 1 (1991); P. Hänggi, P. Talkner and M. Borkovec, *Rev. Mod. Phys.* **62**, 251 (1990).

- [3] For a review of microscopic models that lead to Langevin and generalized Langevin equations see K. Lindenberg and B. J. West, *The Statistical Mechanics of Open and Closed Systems* (VCH Publishers, New York, 1990).
- [4] E. Fermi, J. R. Pasta, and S. M. Ulam, in *Collected Works of Enrico Fermi*, Vol. II (University of Chicago Press, Chicago, 1965), pp. 978-980.
- [5] S. Lepri, R. Livi and A. Politi, Phys. Rev. Lett. **78**, 1896 (1997)
- [6] B. Hu, B. Li and H. Zhao, Phys. Rev. E **57**, 2992 (1998).
- [7] P. Allen and J. Kelner, Am. J. Phys. **66**, 497 (1998).
- [8] R. Bourbonnais and R. Maynard, Phys. Rev. Lett. **64**, 1397 (1990).
- [9] D. Visco and S. Sen, Phys. Rev. E **57**, 224 (1998).
- [10] S. Flach and C. R. Willis, Phys. Rep. **295**, 181 (1998).
- [11] T. Dauxois and M. Peyrard, Phys. Rev. Lett. **70**, 3935 (1993).
- [12] J. Szeftel and P. Laurent, Phys. Rev. E **57**, 1134 (1998).
- [13] G. P. Tsironis and S. Aubry, Phys. Rev. Lett. **77**, 5225 (1996).
- [14] J. M. Bilbault and P. Marquié, Phys. Rev. E **53**, 5403 (1996).
- [15] D. W. Brown, L. J. Bernstein and K. Lindenberg, Phys. Rev. E **54**, 3352 (1996); K. Lindenberg, L. Bernstein and D. W. Brown, in *Stochastic Dynamics*, ed. by L. Schimansky-Geier and T. Peoschel (Springer Lecture Notes in Physics, Springer-Verlag, Berlin, 1997).
- [16] W. Ebeling and M. Jenssen, SPIE **3726**, 112 (1999).
- [17] A. J. Sievers and S. Takeno, Phys. Rev. Lett. **61**, 970 (1988); K. Hori and S. Takeno, J. Phys. Soc. Japan **61**, 2186 (1992); *ibid* 4263; S. Takeno, J. Phys. Soc. Japan **61**, 2821 (1992).
- [18] V. E. Zakharov, Sov. Phys. JEPT **35**, 908 (1972).
- [19] J. F. Lindsner, S. Chandramouli, A. R. Bulsara, M. L. Ocher and W. L. Ditto, Phys. Rev. Lett. **81**, 5048 (1998).

- [20] R. Reigada, A. H. Romero, A. Sarmiento, and K. Lindenberg, *J. Chem. Phys.* **111**, 1373 (1999).
- [21] T. Dauxois, M. Peryard, and A. Bishop, *Phys. Rev. E* **47**, R44 (1993); *ibid* 684.
- [22] F. K. von Gottberg, K. A. Smith, and T. A. Hatton, *J. Chem. Phys.* **108**, 2232 (1998).
- [23] S. P. Plotkin and P. G. Wolynes, *Phys. Rev. Lett.* **80**, 5015 (1998).
- [24] T. Prosen and D. K. Campbell, *chao-dyn/9908021*.
- [25] K. Aoki and D. Kusnezov, *chao-dyn/9910015*
- [26] B. Hu, B. Li, and H. Zhao, *cond-mat/0002192* (to appear in *Phys. Rev. E*).
- [27] K. Lindenberg, D. W. Brown and J. M. Sancho, *FisEs '97, Anales de Física, Monografías RSEF* **4**, 3 (1998).
- [28] W. Ebeling, V. Yu. Podlipchuk, and M. G. Sapeshtinsky, *Int. J. of Bifurcation and Chaos* **8**, 755 (1998).
- [29] J. M. Casado and J. Gómez-Ordóñez, *Phys. Rev. E* **61**, 261 (2000).
- [30] T. Pullerits and V. Sundstrom, *Acc. Chem. Res.* **29**, 381 (1996); X. Hu and K. Schulten, *Physics Today*, 28 (August 1997).
- [31] P. L. Christiansen and A. C. Scott, editors, *Davydov's Soliton Revisited: Self-Trapping of Vibrational Energy in Protein*, NATO ASI Series B: Physics **243** (Plenum Press, New York, 1990).
- [32] K. Bolton, S. Nordholm, and H. W. Schranz, *J. Phys. Chem.* **99**, 2477 (1995).
- [33] L. Cruzeiro-Hansson and S. Takeno, *Phys. Rev. B* **56**, 894 (1997).
- [34] M. A. Collins, *Adv. Chem. Phys.* **53**, 225 (1983); M. A. Collins and D. P. Craig, *Chem. Phys.* **75**, 191 (1983); M. A. Collins, *Phys. Rev. A* **31**, 1754 (1985).
- [35] St. Pnevmatikos, N. Flytzanis, and M. Remoissenet, *Phys. Rev. B* **33**, 2308 (1986).
- [36] See the collection of papers in *Approches microscopique et macroscopique des détonations*, *Journal de physique IV, Colloque C4* **5**, 1155-4339.

- [37] R. Reigada et al., in preparation.
- [38] A. Sarmiento, R. Reigada, A. H. Romero, and K. Lindenberg, *Phys. Rev. E.* **60**, 5317 (1999).
- [39] T. C. Gard, *Introduction to Stochastic Differential Equations*, Marcel Dekker, Vol. 114 of *Monographs and Textbooks in Pure and Applied Mathematics* (1987).
- [40] R. Toral, in *Computational Field Theory and Pattern Formation*, 3rd Granada Lectures in Computational Physics, Lecture Notes in Physics Vol. 448 (Springer Verlag, Berlin, 1995).
- [41] R. Reigada, A. Sarmiento, and K. Lindenberg, in preparation.
- [42] V. I. Melnikov and S. V. Meshkov, *J. Chem. Phys.* **85**, 1018 (1986).
- [43] E. Pollak, H. Grabert and P. Hänggi, *J. Chem. Phys.* **91**, 4073 (1989).
- [44] S. Linkwitz, H. Grabert, E. Turlot, D. Esteve and M. H. Devoret, *Phys. Rev. A* **45**, R3369 (1992).
- [45] R. F. Grote and J. T. Hynes, *J. Chem. Phys.* **73** (1980) 2715.
- [46] J. A. Montgomery, Jr, D. Chandler, and B. J. Berne, *J. Chem. Phys.* **70**, 4056 (1979).
- [47] D. Borgis and M. Moreau, *Mol. Phys.* **57**, 33 (1986).
- [48] D. Kohen and D. J. Tannor, *J. Chem. Phys.* **103**, 6013 (1995).
- [49] J. M. Sancho, A. H. Romero, and K. Lindenberg, *J. Chem. Phys.* **109**, 9888 (1999).
- [50] K. Lindenberg, A. H. Romero, and J. M. Sancho, *Physica D* **133**, 348 (1999).
- [51] R. Reigada, A. H. Romero, K. Lindenberg, and J. M. Sancho, *J. Chem. Phys.* **111**, 676 (1999).
- [52] S. Tucker, *J. Chem. Phys.* **101** (1994) 2006; S. K. Reese, S. Tucker, and G. K. Schenter, *J. Chem. Phys.* **102** (1995) 104.

Figure 1: Schematic of a bistable impurity (“reaction coordinate” RC) connected to a chain that interacts with a heat bath at temperature  $T$ . The chain masses are indicated by rhombuses. Their interactions (shown schematically as springs) may be harmonic or anharmonic. Each mass in the chain is subject to thermal fluctuations denoted by  $\eta$  and the usual accompanying dissipation. The bistable impurity interacts only with the chain, which thus provides its thermal environment. The bistable system is inserted in the chain (“disruptive impurity”); its detailed interaction with the chain is discussed in the text.

Figure 2: Energy (in grey scales) for thermalized chains of 71 oscillators as a function of time. The  $x$ -axis represents the chain and time advances along the  $y$ -axis, with  $t_{max} = 160$ . The temperature is  $k_B T = 0.08$  and the dissipation parameter is  $\gamma = 0.005$ . Top panel: hard chain with  $k = 0.1$ ,  $k' = 1$ ; middle panel: harmonic chain with  $k = 0.1$ ; lower panel: soft chain with  $k = 0.1$ ,  $k' = 5$ .

Figure 3: Transmission coefficient  $\kappa$  vs dissipation parameter  $\gamma_b$  for two temperatures obtained from direct simulation of Eq. (7). Solid circles:  $k_B T = 0.025$ ; triangles:  $k_B T = 0.05$ .

Figure 4: Trajectory of a bistable impurity described by the Langevin equation, Eq. (7). The temperature is  $k_B T = 0.08$ . First panel:  $\gamma_b = 5.0$ . Second panel:  $\gamma_b = 0.02$ . The third (fourth) panel zooms in on a portion of the high-damping (low-damping) trajectory.

Figure 5: Trajectory of a bistable impurity embedded in a chain of 30 oscillators with  $k_B T = 0.08$  and  $\gamma = 0.005$ . Top panel: hard chain with  $k = 0.1$  and  $k' = 1$ . Middle panel: harmonic chain with  $k = 0.1$ . Bottom panel: soft chain with  $k = 0.1$  and  $k' = 5$ .

Figure 6: Trajectory of a bistable impurity embedded in a chain of 30 oscillators. All parameters are the same as in Fig. 5 except that the dissipation parameter has been increased to  $\gamma = 0.05$ .

Figure 7: Correlation functions for the Markovian Kramers problem associated with the trajectories of Fig. 4. Dashed curves:  $\gamma_b = 5.0$ , dotted curves:  $\gamma_b = 0.02$ . First panel: short-time behavior. Second panel: correlation functions on a logarithmic time scale.

Figure 8: Correlation functions associated with the trajectories of Figs. 5 (first panel) and 6 (second panel). Dashed curves: hard chain; solid curves: harmonic chain; dotted curves: soft chain.

Figure 9: Correlation functions for the bistable impurity in the soft chain (first panel) and harmonic chain (second panel) or various values of the dissipation parameter.

Figure 10: Correlation functions for the bistable impurity in the hard chain for various values of the dissipation parameter. First panel: short-time behavior. Second panel: correlation function on a logarithmic scale.